Rabia Malik, Hina Sadaf* and Fiza Dastar

Analysis of Carreau fluid flow by convectively heated disk with viscous dissipation effects

https://doi.org/10.1515/zna-2020-0041 Received February 9, 2020; accepted July 28, 2020; published online September 24, 2020

Abstract: The primary motive of this study is to examine boundary layer flow of Carreau fluid over a convectively heated disk stretching with nonlinear velocity. The flow is assumed to be two dimensional. Moreover, viscous dissipation possessions are taken into description. The dominating nonlinear differential equations involving partial derivatives are changed into nonlinear differential equations involving ordinary derivatives by applying suitable transformations. Numerical outcomes for velocity and temperature are obtained from MATLAB's built-in solver byp4c and presented graphically and in tabular form.

Keywords: Carreau fluid; convective boundary conditions; radially stretching disk; viscous dissipation.

Nomenclature

Velocity component in x direction
 Velocity component in y direction
 Temperature of the fluid

Temperature of the fluid below the sheet

 T_{∞} Ambient fluid temperature

 u_w Stretching velocity along x direction

R_e Local Reynolds number

Ec Eckert number

We Local Weissenberg number τ_w Shear stress of the wall

 μ Thermal viscosity

v Kinematic viscosity of the fluid θ Nondimensional temperature c_p Specific heat at constant pressure

f Dimensionless stream function

m Stretching parameter

 q_w Local heat flux of the surface

*Corresponding author: Hina Sadaf, DBS&H, CEME, National University of Sciences and Technology, Islamabad, Pakistan, E-mail: hsadafqau@gmail.com

Rabia Malik and Fiza Dastar, Department of Mathematics and Statistics, International Islamic University, Islamabad, 44000, Pakistan, E-mail: rabia.malik@iiu.edu.pk (R. Malik), fiza.dastar@gmail.com (F. Dastar)

 h_f Convective heat transfer coefficient

Nu_r Local Nusselt number

Pr Prandtl number

 C_{fr} Local skin friction coefficient γ Generalized Biot number

k Thermal conductivity

ho Fluid density

 η Similarity variable

n Power law index

1 Introduction

Fluid flow owing to stretching boundary is a significant problem in various engineering progressions with solicitations in industries such as extrusion, hot rolling, melt-spinning, wire depiction, glass fiber fabrication, manufacture of plastic and rubber sheets, compression course of metallic plate in a cooling bath and glass and also in polymer industries.

It appears that Sakiadis [1] stood first who described fluid flow motion owing to a stretched surface. After this innovative work, analysis of fluid flow past a stretching sheet has increased inclusive devotion among investigators. The fluid flow problem of Blasius type owing to a stretching sheet has been considered by Crane [2]. Gupta and Gupta [3] prolonged this work with addition of the suction and injection effects. A few other substantial studies connecting to the structures of stretching sheets are discussed by many researchers [4-8]. Turkyilmazoglu [9] explained fluid flow analysis due to a stretching rotating disk in the occurrence of heat transfer and magnetohydrodynamic (MHD). In another paper, Turkyilmazoglu [10] debated combined possessions of flow and heat transfer tempted by two stretchable rotating disks. Eid et al. [11] provided numerical solution for Carreau nanofluid stream problem over a nonlinear stretching surface in the presence of porous medium.

The non-Newtonian fluid flow research has intense attention amongst the researchers because of its diversity of solicitations in engineering, chemical and petroleum industries. The non-Newtonian fluids hypothetically seemed in the engineering of foods, optical fibers, coated sheets, plastic polymers, drilling muds, etc. Due to complexity of the non-Newtonian fluids, a single

constitutive formula is not available in the literature that can be executed to calculate all the assorted possessions of non-Newtonian constituents. The non-Newtonian constitutive equations of fluids are usually with greater order, problematical and are nonlinear in contrast of meek theory of Navier-Stokes. The power-law viscosity model has the constraint, i.e., it cannot be sufficiently expecting the viscosity for very small and large shear rates. Owing to such shortcomings of power law model, constitutive equation of Carreau fluid model [12] depicts both high and low shear rate. Owing to the importance of Carreau fluid model, numerous authors had discussed Carreau fluid model with diverse geometries and with different conventions. Raju and Sandeep [13] discussed Falkner-Skan stream of a magnetic-Carreau fluid past a wedge in the existence of cross diffusion possessions. In another paper, Raju et al. [14] deliberated bioconvection analysis on the nonlinear radiative stream of a Carreau fluid above a stirring wedge with suction or injection. Further studies associated to this spectacle are quoted by studies by Raju et al. [15] and Upadhya et al. [16] and Mamatha Upadhya et al. [17].

Viscous dissipation plays a role of energy source to change temperature distribution, that leads to affected heat transfer rates. The virtue of the outcome of viscous dissipation be contingent on the situation in which the plate is actuality cooled or heated. Orhan et al. [18] examined inspiration of viscous dissipation on heat transfer for a Poiseuille flow. Gireesha et al. [19] explored heat transfers for MHD dusty fluid flow with viscous dissipation due to a stretching sheet. Khan et al. [20] explained heat transfer investigation for magneto hydrodynamics axisymmetric flow concerning stretching disks in the occurrence of Joule heating and viscous dissipation. Influence of unsteady magneto hydrodynamic flow and heat transfer of a fluid over a stretching sheet in the occurrence of heat source and viscous dissipation is discussed by Reddy et al. [21]. For more application about heat transfer reader is referred to mentions [22–30] to the references therein.

The convective heat transfer has gained significance impact in procedures in which high temperatures are convoluted. For example, gas turbines, nuclear plants, storing of thermal energy, etc. Due to numerous manufacturing and industrial techniques of the convective boundary conditions, several investigators have deliberated and stated results on this subject. Bataller [31] analyzed the impact of radiation for the Blasius and Sakiadis flows over the convective boundary surface. Abu Bakar et al. [32] depicted stretching sheet impact under the boundary layer approximation in the occurrence of convective and slip boundary conditions. Makinde and Aziz [33] examined two dimensional boundary layer nano fluid flows past a stretching sheet in the occurrence of convective boundary conditions, and delivered numerical solution for the assumed problem. Besthapu et al. [34] debated stagnation flow of a casson nanofluid owing to a stretching disk comprising the possessions of MHD, convective boundary condition and heat source/sink. Magnetohydrodynamic convective boundary layer flow in the occurrence of slip and heat transfer above nonlinearly stretching pipe surrounded in a thermally stratified intermediate is discussed by Tamoor [35].

In this article, exploration of axisymmetric Carreau fluid flow owing to a convectively heated stretching disk in the existence of viscous dissipation effect is discussed. Resulting coupled equations are resolved numerically by bvp4c. Further, the numerical results are compared to those Khan and Hashim [36]. The profiles of velocity and temperature are presented in graphical form, whereas the results of $Re^{\frac{1}{2}}C_{fr}$ and $Re^{\frac{-1}{2}}Nu_r$ are represented numerically in tabular style.

2 Problem formulation

Assuming the boundary layer axisymmetric flow of Carreau fluid characterized as two-dimensional (r, z), steady and incompressible, generated by convectively heated stretching disk which coincides with z = 0. Here it is considered that the flow is being restricted to z > 0. The nonlinear convectively heated disk has uniform convective temperature T_f along with the ambient fluid temperature T_{∞} $(T_f > T_{\infty})$.

Thus the simplified expressions of the continuity, linear momentum and heat equations in the existence of viscous dissipation after the solicitation of typical boundary layer guesses yield the form as [37]

$$\frac{\partial u}{\partial r} + \frac{\partial w}{\partial z} + \frac{u}{r} = 0,$$
 (1)

$$u\frac{\partial u}{\partial r} + w\frac{\partial u}{\partial z} = v\frac{\partial^{2} u}{\partial z^{2}} \left[1 + \Gamma^{2} \left(\frac{\partial u}{\partial z} \right)^{2} \right]^{\frac{n-1}{2}} + v(n-1)$$

$$\times \left(\frac{\partial u}{\partial z} \right)^{2} \frac{\partial^{2} u}{\partial z^{2}} \left[1 + \Gamma^{2} \left(\frac{\partial u}{\partial z} \right)^{2} \right]^{\frac{n-3}{2}}, \tag{2}$$

$$u\frac{\partial T}{\partial r} + w\frac{\partial T}{\partial z} = \alpha \frac{\partial^2 T}{\partial z^2} + \frac{2\mu}{\rho c_p} \left(\frac{\partial u}{\partial z}\right)^2.$$
 (3)

The associated limitations at the boundary are

$$u(r,0) = U_w = br^m, w(r,0) = 0,$$

$$k\frac{\partial T(r,0)}{\partial z} = -h_f T_f + h_f T(r,0)$$
(4)

$$u(r,\infty) \to 0, T(r,\infty) \to T_{\infty}.$$
 (5)

Introducing the following suitable transformations [37]

$$\eta = zr^{\frac{m-1}{2}} \sqrt{\frac{b(m+1)}{2\nu}}, \quad \Psi = -\sqrt{\frac{2b\nu}{(m+1)}} r^{\frac{m+3}{2}} f(\eta),$$

$$\theta(\eta) = \frac{T - T_{\infty}}{T_f - T_{\infty}},$$
(6)

where η represents the independent variable and $\Psi(r,z)$ the Stroke's stream function which is demarcated as $u = -\frac{1}{r} \left(\frac{\partial \Psi}{\partial z} \right)$ and $w = \frac{1}{r} \left(\frac{\partial \Psi}{\partial r} \right)$, that gives

$$u = U_w f'(\eta)$$
 and

$$w = -r^{\frac{m-1}{2}} \sqrt{\frac{2bv}{(m+1)}} \left[f(\eta) \left(\frac{m+3}{2} \right) + \eta f'(\eta) \left(\frac{m-1}{2} \right) \right]. \quad (7)$$

By means of the above conversions, Eq. (1) is identically contented and Eqs. (2) and (3) are compact to

$$\left[1 + nWe^{2}(f'')^{2}\right]\left[1 + We^{2}(f'')^{2}\right]^{\frac{n-3}{2}}f''' + ff''\left(\frac{m+3}{m+1}\right) - \left(\frac{2m}{m+1}\right)f' = 0,$$
(8)

$$\theta'' + \Pr\left(\frac{m+3}{m+1}\right)\theta' f + Ec(f'')^2 = 0.$$
 (9)

In the above transformed equations the prime symbolizes differentiation w.r.t η , $We\left(=\frac{\Gamma^2 r^{3m-1}b^3m+1)}{2\nu}\right)$ the local Weissenberg number, $Pr\left(=\frac{\mu c_p}{k}\right)$ denotes the Prandtl number and $Ec\left(=\frac{U_w^2}{(T_f-T_\infty)c_p}\right)$ the Eckert number.

The relevant conditions at the boundary reduced to

$$f(\eta) = 0$$
, $f'(\eta) = 1$, $\theta'(\eta) = -\gamma [1 - \theta(\eta)]$, at $\eta = 0$, (10)

$$f'(\eta) \to 0, \quad \theta(\eta) \to 0 \quad \text{as} \quad \eta \to \infty,$$
 (11)

where $y\left(=\frac{h_f}{k}\sqrt{\frac{2\nu}{b(m-1)}}\right)$ indicates the generalized Biot

The physical terms, C_{fr} and Nu_r are illustrated as

$$C_{f_r} = \frac{\tau_w|_{z=0}}{\rho U_{\cdots}^2(r)}, \quad Nu_r = -\frac{rq_w|_{z=0}}{(T_f - T_{\infty})},$$
 (12)

when local shear stress of the wall τ_w and local heat flux of the surface q_w are described by the following expression

$$\tau_{w}|_{z=0} = \eta_{0} \frac{\partial u}{\partial z} \left\{ \left[1 + \Gamma^{2} \left(\frac{\partial u}{\partial z} \right)^{2} \right]^{\frac{n-1}{2}} \right\} \Big|_{z=0},
q_{w}|_{z=0} = -k \left(\frac{\partial T}{\partial z} \right) \Big|_{z=0}.$$
(13)

Thus, using Eqs. (6) and (13) into Eq. (12), we obtain

$$Re^{\frac{1}{2}}C_{f_r} = \sqrt{\frac{m+1}{2}}f''(0)\left[1 + We^2(f''(0))^2\right]^{\frac{n-1}{2}},$$

$$Re^{-\frac{1}{2}}Nu_r = -\sqrt{\frac{m+1}{2}}\theta'(0),$$
(14)

where $Re\left(=\frac{br^{(m+1)}}{v}\right)$ expresses the local Reynolds number.

Solution methodology

The system of BVPs defined by Eqs. (8–11) is first converted into system of IVPs as follows

$$f = y_1, y_1' = y_2, y_2' = y_3,$$

$$y_{3}' = \frac{2m(y_{2}) - y_{1}y_{3}(m+3)}{(m+1)(1+nWe^{2}(y_{3})^{2})(1+We^{2}(y_{3})^{2})^{\frac{n-3}{2}}},$$
(15)

$$\theta = y_4$$
, $\theta' = y_4' = y_5$, $y_5' = -Pry_5y_1\frac{(m+3)}{(m+1)} - Ec(y_3)^2$, (16)

along with conditions

$$y_1(0) = 0$$
, $y_2'(0) = 1$, $y_5(0) = -\gamma + \gamma y_4(0)$. (17)

Afterward, these IVPs are resolved numerically by means of MATLAB's built-in solver bvp4c.

4 Discussion of the results

The main drive of this unit is to discuss the numerical solutions obtained for the profiles of flow and temperature corresponding to distinct values of parameters involving in the equations. Eqs. (8) and (9) along with the conditions defined at the boundaries (10) and (11) are solved by using MATLAB's built-in solver byp4c, numerically. The numerical consequences are explained from Figures 2 to 7 and Tables 1 to 4. The comparison of the values of $Re^{\frac{1}{2}}C_{fr}$ (the local skin friction coefficient) and $Re^{-\frac{1}{2}Nu_r}$ (the local Nusselt number) is also well explained through these tables.

In Tables 1 and 2, we made contrast between our calculated results with those of Khan and Hashim [36] for

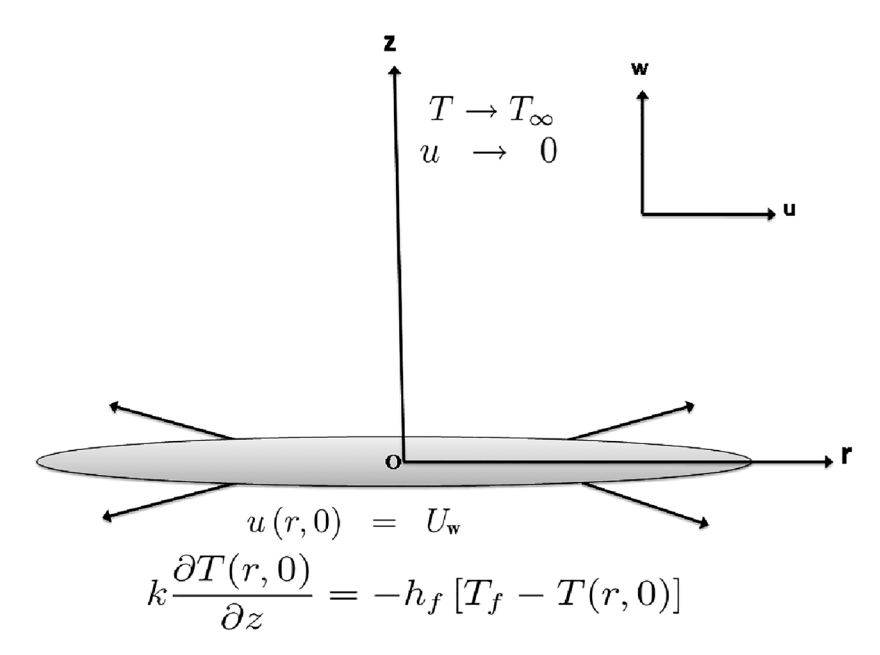


Figure 1: Physical modal of problem.

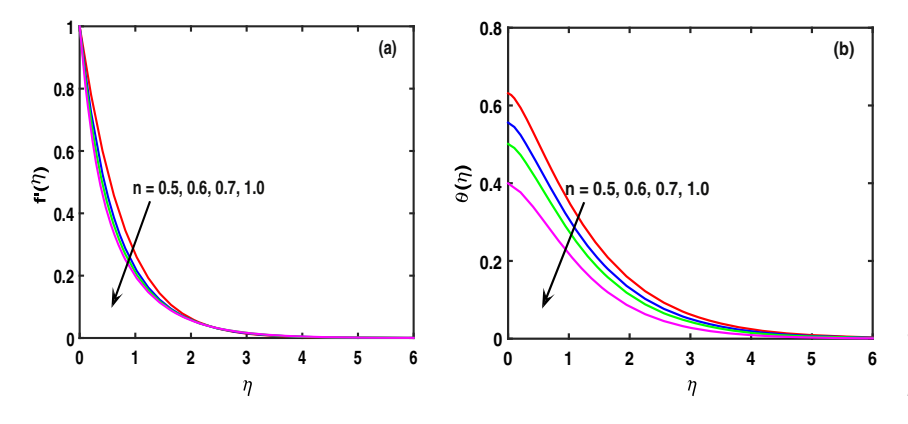


Figure 2 (a, b): The profiles of velocity $f'(\eta)$ and temperature plot $\theta(\eta)$ for several power law index *n* values while We = 3, $\gamma = 0.1$, m = 5.0 and Ec = 0.4 are fixed.

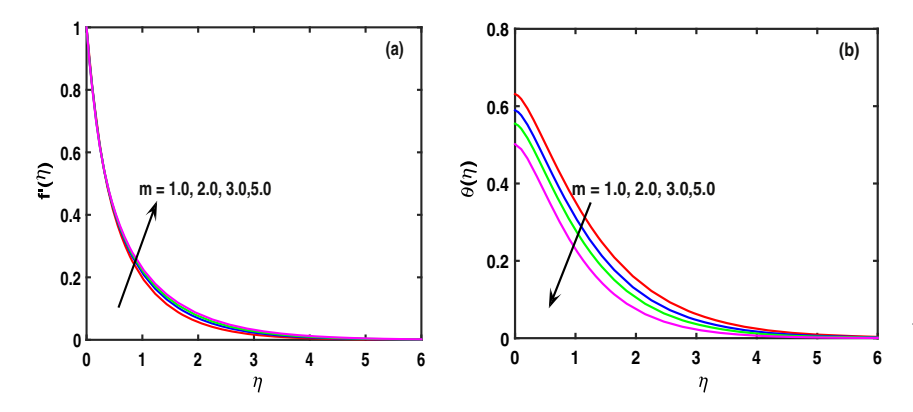


Figure 3 (a, b): The plots of velocity $f'(\eta)$ and temperature $\theta(\eta)$ for several stretching parameter m values when Pr = 1.0, $\gamma = 0.1$, We = 3, Ec = 0.4 and n = 0.5 are fixed.

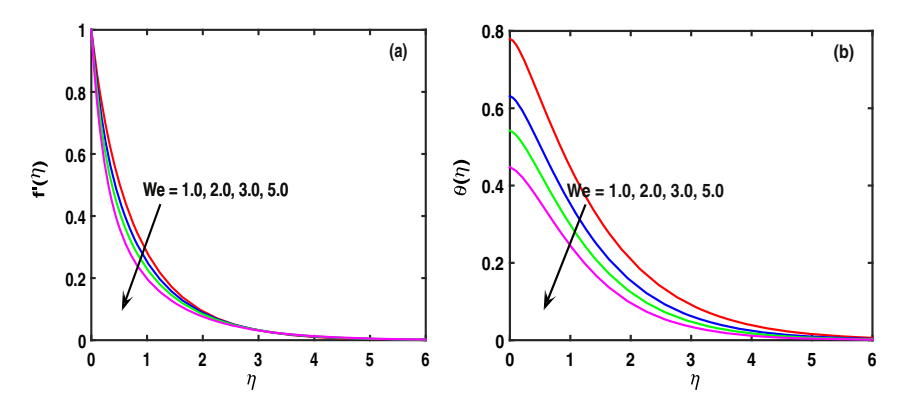


Figure 4(a, b): The diagrams of velocity $f'(\eta)$ and temperature $\theta(\eta)$ for several for several values of We for shear thinning fluid when s = 5, Pr = 1.0, $\gamma = 0.1$, Ec = 0.4 and n = 0.5are fixed.

 $Re^{\frac{1}{2}}C_{fr}$ and $Re^{-\frac{1}{2}}Nu_r$ for various power index *n* values while m = 1 and We = 3 are fixed in order to analyze the efficiency of the current results. The contrast is found to be corrected upto five decimal places. Tables 3 and 4 illustrate the numerical values for $Re^{\frac{1}{2}}C_{fr}$ and $Re^{-\frac{1}{2}}Nu_r$. In Table 3, an increasing behavior of skin friction is clearly shown for increasing power law index n values and stretching parameter *m*, respectively. An increasing behavior in local Nusselt number represented in Table 4 with the increasing n, m, Pr, Ec and y values while it shows a reverse behavior for swelling values of We.

Figure 2a and b depicts the behavior of velocity and temperature plots for power law index n. For increasing the power law index *n* values the velocity profile $f'(\eta)$ increases however, the temperature profile $\theta(\eta)$ is decreasing. Furthermore, both figures demonstrate that thickness of the momentum and thermal boundary layers

in shear thinning fluids is incrementing with an increment in the power index n values.

Figure 3a and b displays the inspiration of velocity and temperature graphs for various values of stretching parameter *m* while considering shear thinning fluids. It is established from these figures that the fluid velocity declines with swelling standards of stretching parameter m for shear thinning fluids (0 < n < 1) and also renowned that large standards of stretching parameter m decreases the thickness of boundary layer. Also, it clearly appears that increasing stretching parameter m values outcomes in an upsurge in the temperature sketch, which promote upturns the boundary layer thickness.

Figure 4a and b illustrates the consequences of the We on the graphs of velocity and temperature for pseudoplastic fluids (0 < n < 1). It can be examine that the profile of velocity is depressed by uplifting the We for shear thinning

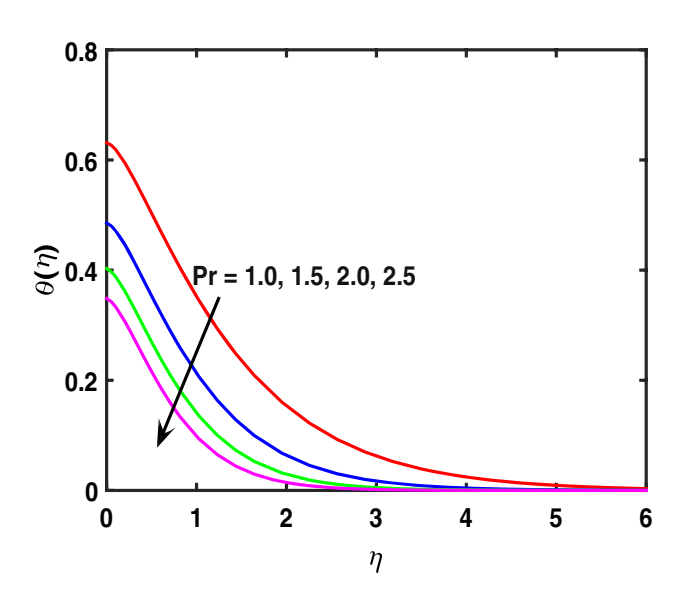


Figure 5: The temperature plot $\theta(\eta)$ for diverse Prandtl number Prvalues when We = 3, m = 5, $\gamma = 0.1$, Ec = 0.4 are fixed.

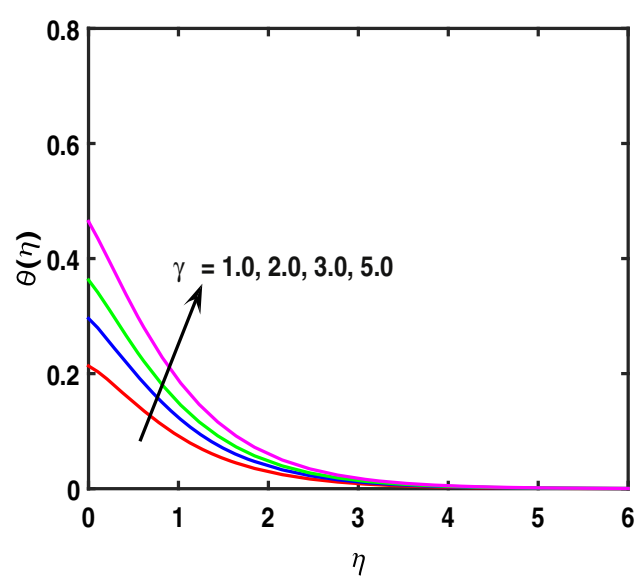


Figure 6: The temperature plot $\theta(\eta)$ for diverse Biot number γ when m = 1, Pr = 1, We = 3 and Ec = 0.1 are fixed.

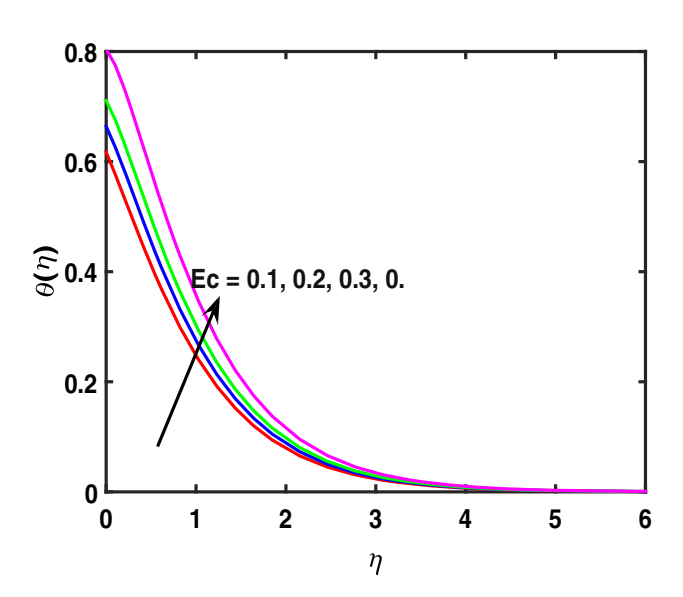


Figure 7: The temperature plot $\theta(\eta)$ for several Eckert number *Ec* values when m=1, Pr=1, We=3 and $\gamma=1$ are fixed.

Table 1: A contrast of the values of local skin friction $Re^{\frac{1}{2}}C_{fr}$ with the obtained results in works for diverse standards of n for m=1 and We=3.0.

		$-Re^{\frac{1}{2}}C_{fr}$		
n	Present study	Khan and Hashim [36]		
0.5	0.8299504	0.829955		
1.0	1.1737218	1.173718		
1.5	1.4524310	1.452433		
2.0	1.6890080	1.689011		
2.5	1.8958584	1.895859		

Table 2: A contrast of Nusselt number $Re^{-\frac{1}{2}}Nu_r$ with the obtained results in literature for diverse values of n for Pr=1, m=1, $\gamma\to\infty$, We=3 and Ec=0.

		$-Re^{-\frac{1}{2}}Nu_r$		
n	Present study	Khan and Hashim [36]		
0.5	0.75284821	0.752 802		
1.0	0.85199807	0.851 995		
1.5	0.91000686	0.910 010		
2.0	0.94657118	0.946 575		
2.5	0.97124077	0.971 246		

fluids because increase in the relaxation time of the fluid generates friction in the fluid particles so, as a result the velocity decreases. However, it is vibrant that for shear

Table 3: Numerical results of $-Re^{\frac{1}{2}}C_{f_r}$ for diverse standards of n We and m.

Fixed parameters	Parameter		$-Re^{\frac{1}{2}}C_{fr}$
We = 3.0, m = 1.0	n	0.5	0.82995
		1.0	1.17372
		1.5	1.45243
		2.0	1.68901
		2.5	1.89586
n = 0.5, $We = 3.0$	m	1.0	0.82995
		2.0	1.04592
		3.0	1.22518
		4.0	1.38159
		5.0	1.52212
m = 1.0, n = 0.5	We	0.5	1.14351
		1.0	1.07288
		2.0	0.92975
		4.0	0.76036
		5.0	0.70876

Table 4: Numerical results of $-Re^{\frac{-1}{2}}Nu_r$ (the local Nusselt number) for diverse *We*, *Ec*, *n*, *y*, *Pr* and *m* values.

Fixed parameters	Parameters		$-Re^{\frac{-1}{2}}Nu_r$
$m = 1.0$, $We = 3.0$, $Ec = 1.0$, $\gamma = 0.5$, $Pr = 1.0$	п	0.5	0.0266878
		0.6	0.2330453
		1.0	0.1231931
$n = 0.5$, $We = 3.0$, $Pr = 1.0$, $Ec = 1.0$, $\gamma = 0.5$	т	1.0	0.0266878
		2.0	0.0634195
		3.0	0.0862917
Pr = 1.0, n = 0.5, m = 1.0, Ec = 1.0, $\gamma = 0.5$	We	0.5	0.1145170
		1.0	0.0915464
		2.0	0.0306914
$n = 0.5$, $m = 1.0$, $We = 3.0$, $Ec = 1.0$, $\gamma = 0.5$	Pr	0.5	0.2094927
		1.0	0.0266878
		1.5	0.0668495
$n = 0.5$, $m = 1.0$, $We = 3.0$, $Ec = 1.0$, $\gamma = 0.5$	Ec	1.0	0.0266878
		2.0	0.3538291
		3.0	0.6809703
n = 0.5, Pr = 1.0, m = 1.0, We = 3.0, Ec = 1.0	γ	0.5	0.0266878
		1.0	0.0381500
		2.0	0.0485833

thinning fluids the temperature graph upsurges with a boost in the $\it We$ values.

Figure 5 shows the temperature profile $\theta(\eta)$ of shear thinning fluids for various Pr values. It is witnessed that

with the swelling of *Pr* values, the profile of temperature declines which causes decline in thickness of thermal boundary layer. Physically, Prandtl number Pr depends upon the thermal diffusivity and larger the Prandtl number Pr values agrees to a weaker thermal diffusivity which creates a reduction in the $\theta(\eta)$ and hence declines the thickness of thermal boundary layer.

Significance of temperature distribution $\theta(\eta)$ for Biot number y is accessible in Figure 6. It appears from this figure that the higher standards of Biot number y corresponds to development in the temperature graph, as well as the thickness of thermal boundary layer. Figure 7 depicts the variation in $\theta(\eta)$ for various Eckert number *Ec* values. It is perceived that swelling of the Eckert number *Ec* values enhances the thickness of thermal boundary layer.

5 Deductions

In this article, a flow analysis of Carreau fluid over a convectively heated disk was investigated. We concluded that momentum boundary layer thickness upsurges and thermal boundary layer thickness declines for the swelling standards of the power law index n. Swelling the Weissenberg number We concentrated the scale of the fluid velocity for shear thinning. The temperature and thermal boundary layer thickness was low by swelling the Prandtl number Pr. The thermal boundary layer thickness was amplified with the swelling standards of Biot number y and Eckert number Ec.

Author contribution: All the authors have accepted responsibility for the entire content of this submitted manuscript and approved submission.

Research funding: None declared.

Conflict of interest statement: The authors declare no conflicts of interest regarding this article.

References

- [1] B. C. Sakiadis, "Boundary-layer behavior on continuous solid surfaces: I. Boundary-layer equations for two-dimensional and axisymmetric flow," AIChE J., vol. 7, p. 26, 1961.
- [2] L. J. Crane, "Flow past a stretching plate," Z. Angew. Math. Phys. ZAMP, vol. 21, p. 645, 1970.
- [3] P. S. Gupta and A. S. Gupta, "Heat and mass transfer on a stretching sheet with suction or blowing," Can. J. Chem. Eng., vol. 55, p. 744, 1977.
- [4] Ahmed. F. Al-Hossainy, M. R. Eid, and M. Sh Zoromba, Phys. Scr. https://doi.org/10.1088/1402-4896/ab2413.

- [5] M. Eid, "Time-dependent flow of water-NPs over a stretching sheet in a saturated porous medium in the stagnation-point region in the presence of chemical reaction," J. Nanofluids, vol. 6, p. 550, 2017.
- [6] C. S. K. Raju and N. Sandeep, "Unsteady three-dimensional flow of Casson-Carreau fluids past a stretching surface," Alex. Eng. J., vol. 55, p. 1115, 2016.
- [7] S. U. Mamatha, Mahesha, C. S. K. Raju, and O. D. Makinde, "Effect of Convective Boundary Condition on MHD Carreau Dusty Fluid over a Stretching Sheet with Heat Source," Defect Diffus. Forum, vol. 377, p. 233, 2017.
- [8] M. R. Eid, K. L. Mahny, A. Dar, and T. Muhammad, "Numerical study for Carreau nanofluid flow over a convectively heated nonlinear stretching surface with chemically reactive species," Phys. A Stat. Mech. Appl., vol. 540, p. 123063, 2020.
- [9] M. Turkyilmazoglu, "MHD fluid flow and heat transfer due to a stretching rotating disk," Int. J. Therm. Sci., vol. 51, p. 195, 2012.
- [10] M. Turkyilmazoglu, "Flow and heat simultaneously induced by two stretchable rotating disks," Phys. Fluids, vol. 28, p. 043601, 2016.
- [11] M. R. Eid, K. L. Mahny, T. Muhammad, and M. Sheikholeslami, "Numerical treatment for Carreau nanofluid flow over a porous nonlinear stretching surface," Results Phys., vol. 8, p. 1185, 2018.
- [12] RVMSSK. Kumar, GV. Kumar, C.S. K. Raju, S.A. Shehzad, and S. V. K. Varma, "Analysis of Arrhenius activation energy in magnetohydrodynamic Carreau fluid flow through improved theory of heat diffusion and binary chemical reaction," J. Phys. Commun., vol. 2, p. 035004, 2018.
- [13] C. S. K. Raju and N. Sandeep, "Falkner-Skan flow of a magnetic-Carreau fluid past a wedge in the presence of cross diffusion effects," Eur. Phys. J. Plus., vol. 131, p. 267, 2016.
- [14] C. S. K. Raju, S. M. Ibrahim, and S. Anuradha, "Bio-convection on the nonlinear radiative flow of a Carreau fluid over a moving wedge with suction or injection," Eur. Phys. J. Plus., vol. 131, p. 409, 2016.
- [15] C. S. K. Raju, M. M. Hoque, N. N. Anika, and S. U.P. Sharma, "Natural convective heat transfer analysis of MHD unsteady Carreau nanofluid over a cone packed with alloy nanoparticles," Powder Technol., vol. 317, p. 408, 2017.
- [16] S. M. Upadhya, C. S. K. Mahesha, and C. S. K. Raju, "Multiple slips on magnetohydrodynamic Carreau dustynano fluid over a stretched surface with Cattaneo-Christov heat flux," J. Nanofluids, vol. 6, p. 1074, 2017.
- [17] S. Mamatha Upadhya, Mahesha, and C. S. K. Raju, "Unsteady flow of Carreau fluid in a suspension of dust and graphene nanoparticles with Cattaneo-Christov heat flux," J. Heat Transfer., vol. 140, p. 092401, 2018.
- [18] A. Orhan and A. Mete, "Viscous-dissipation effects on the heat transfer in a Poiseuille flow," Applied Energy, vol. 83, p. 495, 2006.
- [19] B. J. Gireesha, G. K. Ramesh, and C. S. Bagewadi, "Heat transfer in MHD flow of a dusty fluid over a stretching sheet with viscous dissipation," Adv. Appl. Sci. Res., vol. 3, no. 4, pp. 2392-2401,
- [20] N. Khan, M. Sajid, and T. Mahmood, "Heat transfer analysis for magnetohydrodynamics axisymmetric flow between stretching disks in the presence of viscous dissipation and Joule heating," AIP Adv., vol. 5, p. 057115, 2015.

- [21] M. G. Reddy, P. Padma, and B. Shankar, "Effects of viscous dissipation and heat source on unsteady MHD flow over a stretching sheet," Ain Shams Eng. J., vol. 6, p. 1195, 2015.
- [22] M. Sheikholeslami, "New computational approach for exergy and entropy analysis of nanofluid under the impact of Lorentz force through a porous media," Comput. Methods Appl. Mech. Eng., vol. 344, p. 319, 2019.
- [23] M. Sheikholeslami, B. Rezaeianjouybari, M. Darzi, A. Shafee, and Z.T. K. Nguyen, "Application of nano-refrigerant for boiling heat transfer enhancement employing an experimental study," Int. J. Heat Mass Transfer, vol. 141, p. 974, 2019.
- [24] S. Lahmar, M. Kezzar, M. R. Eid, and M. R. Sari, "Heat transfer of squeezing unsteady nanofluid flow under the effects of an inclined magnetic field and variable thermal conductivity," Phys. A Stat. Mech. Appl., vol. 540, p. 123138, 2020.
- [25] M. R. Eid, A. F. Al-Hossainy, and M. S. Zoromba, "FEM for bloodbased SWCNTs flow through a circular cylinder in a porous medium with electromagnetic radiation," Commun. Theor. Phys., vol. 71, p. 1425, 2019.
- [26] C. S. K. Raju and N. Sandeep, "A comparative study on heat and mass transfer of the Blasius and Falkner-Skan flow of a bioconvective Casson fluid past a wedge," Eur. Phys. J. Plus., vol. 131, p. 405, 2016.
- [27] C. S. K. Raju, S. Saleem, S. U. Mamatha, and I. Hussain, "Heat and mass transport phenomena of radiated slender body of three revolutions with saturated porous: Buongiorno's model," Int. J. Therm. Sci., vol. 132, p. 309, 2018.
- [28] C. S. K. Raju and N. Sandeep, "MHD slip flow of a dissipative Casson fluid over a moving geometry with heat source/sink: A numerical study," Acta Astron., vol. 133, p. 436, 2017.
- [29] B. Rezaeianjouybari, M. Sheikholeslami, and A.H. Babazadeh, "A novel Bayesian optimization for flow condensation

- enhancement using nanorefrigerant: a combined analytical and experimental study," Chem. Eng. Sci., vol. 215, p. 115465, 2020.
- [30] M. Sheikholeslami, M. A. Sheremet, and A.I. Tlili, "Simulation of nanoliquid thermogravitational convection within a porous chamber imposing magnetic and radiation impacts," Phys. A Stat. Mech. Appl., vol. 550, p. 124058, 2020.
- [31] R. C. Bataller, "Radiation effects for the Blasius and Sakiadis flows with a convective surface boundary condition," Appl. Math. Comput., vol. 206, p. 832, 2008.
- [32] N. A. Abu Bakar, W. M. K. A. W. Zaimi, R. A. Hamid, B. Bidin, and A. Ishak, "Applications of Runge-Kutta-Fehlberg Method and Shooting Technique for Solving Classical Blasius Equation," World Appl. Sci. J., vol. 17 (Special Issue of Applied Math), pp. 10-15, 2012.
- [33] O. D. Makinde and A. Aziz, "Boundary layer flow of a nanofluid past a stretching sheet with a convective boundary condition," Int. J. Therm. Sci., vol. 50, p. 1326, 2011.
- [34] P. Besthapu, B. Shankar, and Kishore, "MHD stagnation point flow of a Casson Nanofluid towards a radially stretching disk with convective boundary condition in the presence of heat source/sink," J. Nanofluids., vol. 5, p. 1, 2016.
- [35] M. Tamoor, "MHD convective boundary layer slip flow and heat transfer over nonlinearly stretching cylinder embedded in a thermally stratified medium," Resul. Phys., vol. 7, p. 4247, 2017.
- [36] M. Khan and J. Hashim, "Axisymmetric flow and heat transfer of the Carreau fluid due to a radially stretching sheet: Numerical study," J. Appl. Mech. Tech. Phys., vol. 58, p. 410,
- [37] G. Radha, N. B. Reddy, K. Gangadhar, and S. S. Reddy, "Slip flow and convective heat transfer of the Carreau Fluid over a radially stretching sheet," IJMTT, vol. 54, p. 4, 2018.